

Structural Isomers of S<sub>2</sub>N<sub>2</sub>

D. Scott Warren, Ming Zhao, and Benjamin M. Gimarc\*

Contribution from the Department of Chemistry and Biochemistry, University of South Carolina, Columbia, South Carolina 29208

Received August 5, 1994<sup>⊗</sup>

**Abstract:** The variety of structures observed for tetraatomic molecules containing 22 valence electrons suggests an energy surface with a number of minima of comparable depths. For S<sub>2</sub>N<sub>2</sub> we have carried out geometry optimized SCF MO RHF/6-31G\* calculations and located 9 minima, 7 of which are also minima at the MP2 level. The three lowest energy structures are the linear chain SNSN and the two 4-membered rings SNSN and SNNS. At both RHF and MP2 levels and using basis sets that include additional d-type and even f-type polarization functions as well as diffuse functions, these three structures are real minima on the energy surface. At this level of theory, the three structures are too close in energy to allow us to pick the global minimum. The structure well characterized by experiment is the alternant ring SNSN. Its existence can be rationalized as a result of the method of preparation. A calculated vibrational frequency for the pairwise ring SNNS closely matches that of the vibrational absorption peak that Hassanzadeh and Andrews have attributed to a new isomer of S<sub>2</sub>N<sub>2</sub> which they claim to have produced in matrix isolation experiments. Calculated bond distances in the three low energy isomers can be rationalized by traditional VB and MO models. Qualitative MO arguments are used to evaluate processes by which SN fragments might dimerize to form the SNSN chain and the two rings and to rationalize an activation barrier separating chain and ring.

## Introduction

Figure 1 displays a selection of tetraatomic molecules and ions of the main-group elements containing 22 valence electrons and whose structures have been determined experimentally. X-ray crystal structure analysis shows that S<sub>2</sub>N<sub>2</sub> is a very nearly square-planar ring with equivalent S–N bonds.<sup>1,2</sup> The homoatomic dications S<sub>4</sub><sup>2+</sup>, Se<sub>4</sub><sup>2+</sup>, and Te<sub>4</sub><sup>2+</sup> also have square-planar structures.<sup>3–5</sup> In these rings, six valence electrons occupy  $\pi$  MOs, a set of orbitals that are antisymmetric with respect to reflection in the plane of the ring. These features of their molecular and electronic structures have given rise to considerable speculation about whether the square-planar rings are aromatic.<sup>6–10</sup> The rotational spectrum of N<sub>2</sub>O<sub>2</sub> reveals this molecule to be a loose dimer in which the two NO units are connected by a weak N–N bond to form a planar cis chain.<sup>11</sup> P<sub>2</sub>O<sub>2</sub> has been generated and trapped in rare gas matrices.<sup>12</sup> The PO stretching frequency assigned to P<sub>2</sub>O<sub>2</sub> agrees with that obtained from ab initio calculations assuming a symmetrical

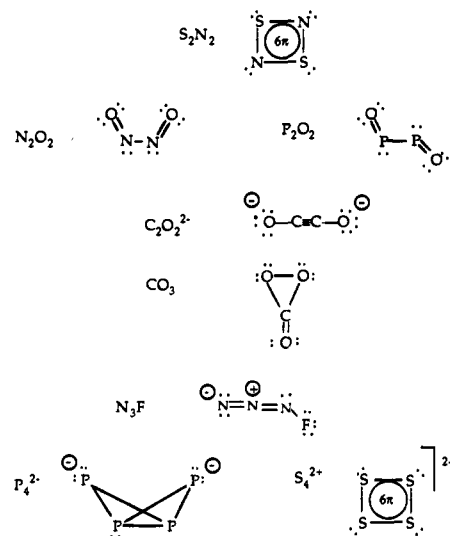


**Figure 1.** Some of the known 22 valence electron molecules and ions. The variety of structures suggests an energy surface with many minima.

planar trans structure for OPPO.<sup>13</sup> X-ray diffraction of K<sub>2</sub>C<sub>2</sub>O<sub>2</sub> crystals shows a linear OCCO<sup>2-</sup> dianion with a C≡C triple bond as would also be expected in the dihaloacetylenes.<sup>14</sup> CO<sub>3</sub> has been identified among the microwave discharge products trapped in rare gas matrices. The infrared spectrum points to a Y or Lacrosse stick shape for CO<sub>3</sub><sup>15,16</sup> but another view prefers a chain-type structure.<sup>17</sup> CS<sub>3</sub> is believed to be Y shaped also.<sup>18–20</sup>

- (13) Lohr, L. L. *J. Phys. Chem.* **1990**, *94*, 1807. Bruna, P. J.; Mühlhäuser, M.; Peyerimhoff, S. D. *Chem. Phys. Lett.* **1991**, *180*, 606.  
 (14) Weiss, E.; Buchner, W. *Helv. Chim. Acta* **1963**, *46*, 1121.  
 (15) Moll, N. G.; Clutter, D. R.; Thompson, W. E. *J. Chem. Phys.* **1966**, *45*, 4469.  
 (16) Jacox, M. E.; Milligan, D. E. *J. Chem. Phys.* **1971**, *54*, 919.  
 (17) LaBonville, P.; Kugel, R.; Ferraro, J. R. *J. Chem. Phys.* **1977**, *67*, 1477.  
 (18) Basco, N.; Pearson, E. A. *Trans. Faraday Soc.* **1967**, *63*, 2684.

- <sup>⊗</sup> Abstract published in *Advance ACS Abstracts*, October 1, 1995.  
 (1) Mikulski, C. M.; Russo, P. J.; Saran, M. S.; MacDiarmid, A. G.; Garito, A. F.; Heeger, A. J. *J. Am. Chem. Soc.* **1975**, *97*, 6358.  
 (2) Cohen, M. J.; Garito, A. F.; Heeger, A. J.; MacDiarmid, A. G.; Mikulski, C. M.; Saran, M. S.; Kleppinger, J. *J. Am. Chem. Soc.* **1976**, *98*, 3844.  
 (3) Passmore, J.; Sutherland, G.; White, P. S. *J. Chem. Soc., Chem. Commun.* **1980**, 330.  
 (4) Brown, I. D.; Crump, D. B.; Gillespie, R. J. *Inorg. Chem.* **1971**, *10*, 2319. Cardinal, G.; Gillespie, R. J.; Sawyer, J. F.; Vekris, J. F. *J. Chem. Soc., Dalton Trans.* **1982**, 765.  
 (5) Couch, T. W.; Lokken, D. A.; Corbett, J. D. *Inorg. Chem.* **1972**, *11*, 357. Beck, J. Z. *Naturforsch.* **1990**, *458*, 1610.  
 (6) Banister, A. J. *Nature Phys. Sci.* **1972**, *237*, 92.  
 (7) Gimarc, B. M.; Trinajstić, N. *Pure Appl. Chem.* **1980**, *52*, 1443.  
 (8) Gimarc, B. M. *Pure Appl. Chem.* **1990**, *62*, 423.  
 (9) Jafri, J. A.; Newton, M. D.; Pakkanen, T. A.; Whitten, J. L. *J. Chem. Phys.* **1977**, *66*, 5167.  
 (10) Janssen, R. A. J. *J. Phys. Chem.* **1993**, *97*, 6384.  
 (11) Kukolich, S. G. *J. Am. Chem. Soc.* **1982**, *104*, 4715.  
 (12) Mielke, Z.; McCluskey, M.; Andrews, L. *Chem. Phys. Lett.* **1990**, *165*, 146.

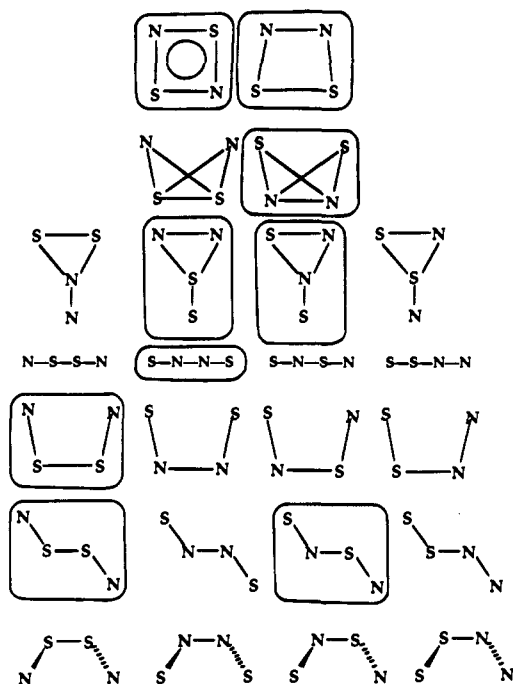


**Figure 2.** The 24 structures chosen as starting shapes for RHF/6-31G\* geometry optimizations. The enclosed structures represent real minima at this level of theory.

Structures related to  $P_4^{2-}$  are butterfly shaped, two non-coplanar triangles that share a common edge.<sup>21,22</sup> The microwave structure of  $N_3F$  is a chain with the fluorine atom bent at an angle to the axis of a nearly linear  $N_3$  unit.<sup>23</sup>

Chemists often assume that molecules composed of the same number of similar kinds of atoms and containing the same number of valence electrons have similar electronic structures and therefore similar molecular shapes. Indeed, many isoelectronic series demonstrate this rule.<sup>24</sup> The variety of different structures taken on by members of the 22-electron tetraatomic series suggests an energy surface with a number of relative minima that are rather close in energy. In an attempt to explore this energy surface, we have carried out ab initio SCF MO calculations at several levels of approximation for  $S_2N_2$  in different structural forms. We chose to investigate  $S_2N_2$  because Hassanzadeh and Andrews have recently reported matrix isolation infrared spectra that seem to point to the existence of a new structural isomer of  $S_2N_2$ .<sup>25</sup>

### Calculations

Figure 2 shows 24 shapes for which we attempted geometry optimized RHF/6-31G\* calculations using the GAUSSIAN 92 program package.<sup>26,27</sup> The asterisk here indicates that the basis set includes a set of d-type polarization functions on each atom. Our experience and

(19) Arnold, S. J.; Brownlee, W. G.; Kimball, G. H. *J. Phys. Chem.* **1970**, *74*, 8.

(20) Breckenridge, W. H.; Taube, H. *J. Chem. Phys.* **1970**, *53*, 1750.

(21) Niecke, E.; Ruger, R.; Krebs, B. *Angew. Chem., Int. Ed. Engl.* **1982**, *21*, 544.

(22) Riedel, R.; Hansen, H.-D.; Fluck, E. *Angew. Chem., Int. Ed. Engl.* **1985**, *24*, 1056.

(23) Christen, D.; Mack, H. G.; Schatte, G.; Willner, H. *J. Am. Chem. Soc.* **1988**, *110*, 707.

(24) Gimarc, B. M. *Molecular Structure and Bonding: The Qualitative Molecular Orbital Approach*; Academic Press: New York, 1979.

(25) Hassanzadeh, P.; Andrews, L. *J. Am. Chem. Soc.* **1992**, *114*, 83.

(26) GAUSSIAN 92, Revision C.4, Frisch, M. J.; Trucks, G. W.; Head-Gordon, M.; Gill, P. M. W.; Wong, M. W.; Foresman, J. B.; Johnson, B. G.; Schlegel, H. B.; Robb, M. A.; Replogle, E. S.; Gomperts, R.; Andres, J. L.; Raghavachari, K.; Binkley, J. S.; Gonzales, C.; Martin, R. L.; Fox, D. J.; Defrees, D. J.; Baker, J.; Stewart, J. J. P.; Pople, J. A.; Gaussian, Inc., Pittsburgh: PA 1992.

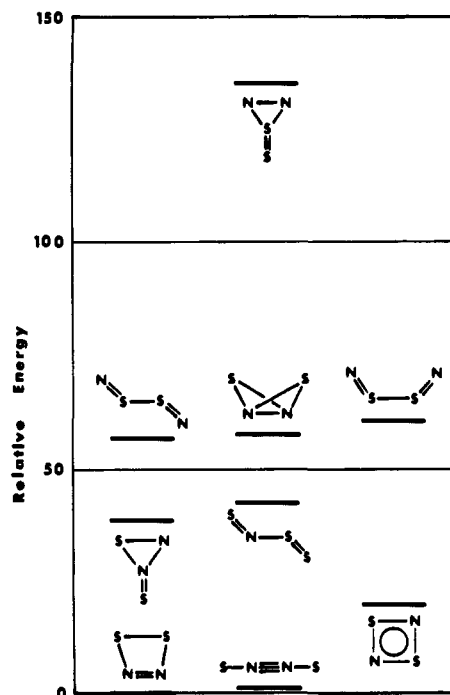


**Figure 3.** Relative energies of structures corresponding to real minima on the RHF/6-31G\* energy surface.

that of many others shows that polarization functions are necessary in order to describe adequately structural details of molecules that contain atoms of elements of the second row of the periodic table.<sup>28-33</sup> Although we initiated geometry searches with a limited number of the possible shapes available to 4-connected atoms, we could draw conclusions about the relative stabilities of a larger set of shapes because several of the calculations were performed with rather low symmetry restrictions which in principle allowed access to other, higher symmetry structures. For example, it would have been possible for the butterfly structures to convert to a tetrahedron, a planar rhombus, or a nonplanar, puckered square had energy minima been located in those directions. The Y-shaped structures might have opened, breaking the bond linking the two equivalent peripheral atoms, to give a planar triangular structure. At the RHF/6-31G\* level, we found that the planar cis form of  $SNNS$  closes to the  $SNNS$  ring and all the nonplanar gauche shapes collapsed to yield planar cis or trans structures.

Vibrational frequencies calculated at the RHF/6-31G\* level of theory identified 9 relative minima on the  $S_2N_2$  surface. These structures are enclosed in boxes in Figure 2. Relative energies corresponding to these minima are displayed in Figure 3, from which one can see that 8 of the 9 minima are within 60 kcal/mol of each other. The  $SN=NS$  linear chain and the planar pairwise ring  $SNNS$  have essentially the same energies at the low end of the energy ordering. The planar alternant ring  $SNSN$ , known and well characterized experimentally, lies almost 20 kcal/mol higher.

To get an appreciation of the effects of electron correlation in some of the lower energy structures, we carried out CISD, MP2, and MP4SDTQ/6-31G\* calculations,<sup>27</sup> but using geometries determined by RHF/6-31G\* optimizations for the five structures of lowest energy in Figure 3. The relative energies of these structures at the various levels of approximation are compared in Figure 4. Electron correlation pulls

(27) Hehre, W. J.; Radom, L.; Schleyer, P. v. R.; Pople, J. A. *Ab Initio Molecular Orbital Theory*; Wiley: New York, 1986.

(28) Collins, M. P. S.; Duke, B. J. *J. Chem. Soc., Chem. Commun.* **1976**, 701.

(29) Gimarc, B. M.; Warren, D. S. *Inorg. Chem.* **1991**, *30*, 3276.

(30) Warren, D. S.; Gimarc, B. M. *J. Am. Chem. Soc.* **1992**, *114*, 5378.

(31) Warren, D. S.; Gimarc, B. M. *J. Phys. Chem.* **1993**, *97*, 4031.

(32) Trinquier, G.; Daudey, J.-P.; Komiha, N. *J. Am. Chem. Soc.* **1985**, *107*, 7210.

(33) Raghavachari, K.; Haddon, R. C.; Binkley, J. S. *Chem. Phys. Lett.* **1985**, *122*, 219.

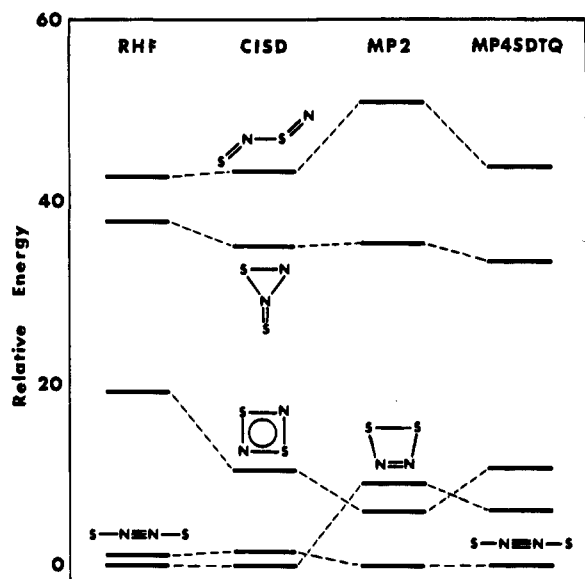


Figure 4. Relative energies of low-energy structures from different levels of theory (but at RHF/6-31G\* geometries) including some effects of electron correlation.

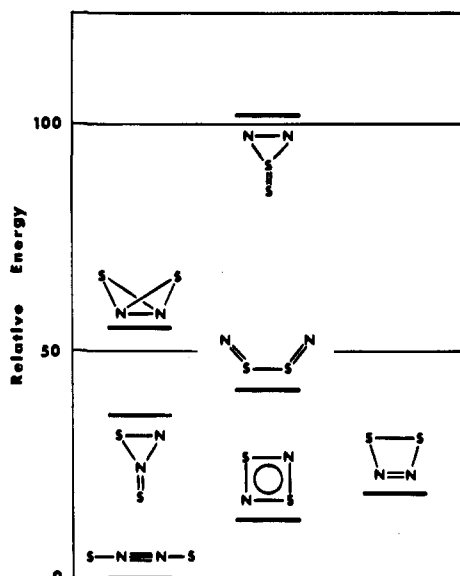


Figure 5. Relative energies of structures corresponding to real minima on the MP2/6-31G\* energy surface. This is a subset of structures from Figure 3.

the SNNS linear chain and the two 4-membered rings to within 10 kcal/mol of each other. Other structures are at much higher energies.

To determine the effects of both electron correlation and geometry optimization, we carried out geometry optimized MP2/6-31G\* calculations for the 9 structures which correspond to real minima at the RHF/6-31G\* level. Relative energies are shown in Figure 5. Calculated vibrational frequencies indicate that at least 7 of the 9 structures are real minima on the MP2/6-31G\* surface. During optimization, the trans SNNS chain separated into two widely spaced NS units. The planar trans SNNS chain is not a real minimum under  $C_2$  symmetry constraints. The structure with the lowest energy on the MP2/6-31G\* surface is the SNNS linear chain. But the structure is not strictly linear, the sulfurs being bent trans from linearity by  $0.15^\circ$ . The energy of this slightly bent structure is lower than that of the exactly linear chain by only  $10^{-5}$  hartree. Therefore in the following discussion, we continue to refer to this structure as the SNNS linear chain. Although their relative energies change compared to RHF and even single-point MP2 results, the linear chain and the two 4-membered rings remain considerably lower in energy than any of the others.

In an attempt to resolve the relative energies of the three low-energy structures, the linear SNNS chain and alternant and nonalternant rings,

we carried out calculations with four different basis sets. For each atom, Set A (=6-31G\*) has a split valence shell plus a set of d-type polarization functions. Set B (=6-311++G\*) has a triply-split or triple- $\zeta$  valence shell, two diffuse functions, and a set of d-functions. Set C (=6-311G(2df)) has a triple valence shell, two sets of d-functions, and one set of f-functions. Set D (=6-311++G(3df)) contains the triple valence shell, two diffuse functions, three sets of d-functions, and a set of f-functions. Table 1 contains total energies of the three low-energy structures. We report MP2 energies calculated at corresponding RHF geometries for A, B, C, and D. For basis sets A, C, and D, we give geometry optimized energies at the MP2 level. To make trends more apparent, we have plotted in Figure 6 the relative energies of the three low-energy structures as functions of basis set improvement and electron correlation corrections to the MP2 level. At the RHF level, the order of stabilities is the same for all four basis sets, the nonalternant ring being the most stable and the alternant ring the least stable. Augmentation of the basis set by f- and additional d-type polarization functions considerably lowers the relative energy of the alternant ring and, to a lesser extent, that of the nonalternant ring. Inclusion of MP2 corrections at RHF geometries also rearranges the relative energies. At this level, electron correlation shifts the nonalternant ring to the high-energy position and the SNNS chain now has the lowest energy. Addition of f- and extra d-type functions stabilizes the alternant ring, giving it the lowest energy with basis sets C and D. With geometry optimization at the MP2 level for basis sets C and D, the linear SNNS chain and the alternant ring have virtually identical energies. At the highest level of theory considered here, MP2/6-311++G(3df), the two rings and the linear SNNS chain are within 12 kcal/mol of each other.

In a final attempt to discover which structure is the global minimum, we performed calculations at the MP4SDTQ level but with MP2 geometries for basis set C (Table 1). The results give the linear SNNS chain the lowest energy with alternant and nonalternant rings 4.9 and 9.3 kcal/mol, respectively, above it. We do not feel that we have sufficient justification for claiming that a particular structure constitutes the global minimum, but we can conclude that these structures are real minima and relatively close in energy.

Many other investigators have reported calculations for  $S_2N_2$  in one or more structural forms. We mention only these studies that are closely related to the work we present here. Haddon, Wasserman, and co-workers<sup>34</sup> carried out RHF calculations with STO-2G, STO-3G, and 4-31G basis sets and geometry optimization for the two 4-membered rings, the SNNS linear chain, and the N-N connected butterfly. Collins and Duke<sup>28</sup> used a basis set containing polarization functions to do SCF calculations for the two 4-membered rings and bent NS-SN and SN-SN chains. They found the alternant ring SNSN to have much the lowest energy. Janssen<sup>10</sup> reports RHF and MP2 calculations with the 6-31G\* basis set for the alternant ring and RHF/6-31G\* results for the N-N connected butterfly. As they must, our results for these isomers match Janssen's exactly. Palmer and Guest used a double- $\zeta$  basis set with polarization functions to do calculations for the alternant ring.<sup>35</sup> Finally, we mention MNDO and AM1 calculations performed by Jones and Bardo for the two 4-membered rings.<sup>36</sup> Both semiempirical methods show the pairwise ring to be more stable than the alternant ring. Our investigation surpasses all previous studies in the number of different structures surveyed, extent of basis sets employed, and level of electron correlation corrections included.

### Structural Parameters

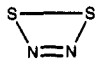

Figure 7 presents calculated bond distances obtained from various levels of theory for the three low-energy structures. Figure 8 contains selected structural parameters for the remaining six higher-energy structures that we found to be real minima on the RHF/6-31G\* energy surface. For comparison, Table 2 lists typical NN, NS, and SS bond distances from a variety of experimental sources. The alternant ring SNSN (Figure 7)

(34) Haddon, R. C.; Wasserman, S. R.; Wudl, F.; Williams, G. R. *J. Am. Chem. Soc.* **1980**, *102*, 6687.

(35) Palmer, M. H.; Guest, M. F. *Chem. Phys. Lett.* **1986**, *110*, 187.

(36) Jones, W. H.; Bardo, R. D. *J. Phys. Chem.* **1993**, *97*, 4973.

**Table 1.** Total Energies (hartrees) of the Three Low-Energy S<sub>2</sub>N<sub>2</sub> Structures Calculated at Various Levels of Approximation<sup>a</sup>

method/basis set/geometry	total energy (relative energy)		
		S-N=N-S	
A: MP2/6-31G*/RHF	904.375 11 (9.0)	904.389 49 (0)	904.380 00 (6.0)
MP4SDTQ/6-31G*/RHF	904.428 99 (6.1)	904.438 66 (0)	904.421 48 (10.8)
MP2/6-31G*	904.410 00 (18.5)	904.439 46 (0)	904.419 92 (12.3)
MP4SDTQ/6-31G*/MP2	904.461 31 (13.7)	904.483 08 (0)	904.462 16 (13.1)
B: MP2/6-311++G*/RHF	904.477 30 (8.1)	904.490 19 (0)	904.481 83 (5.2)
C: MP2/6-311G(2df)/RHF	904.629 69 (9.0)	904.637 21 (4.3)	904.644 10 (0)
MP4SDTQ/6-311G(2df)/RHF	904.698 02 (3.5)	904.703 60 (0)	904.699 84 (2.4)
MP2/6-311G(2df)	904.635 87 (12.5)	904.655 86 (0)	904.653 18 (1.7)
MP4SDTQ/6-311G(2df)/MP2	904.703 50 (9.3)	904.718 34 (0)	904.710 61 (4.9)
D: MP2/6-311++G(3df)/RHF	904.649 64 (10.7)	904.655 58 (7.0)	904.666 74 (0)
MP2/6-311++G(3df)	904.656 12 (11.8)	904.674 73 (0.2)	904.674 98 (0)

<sup>a</sup> The relative energy (kcal/mol) appears in parentheses following the total energy.

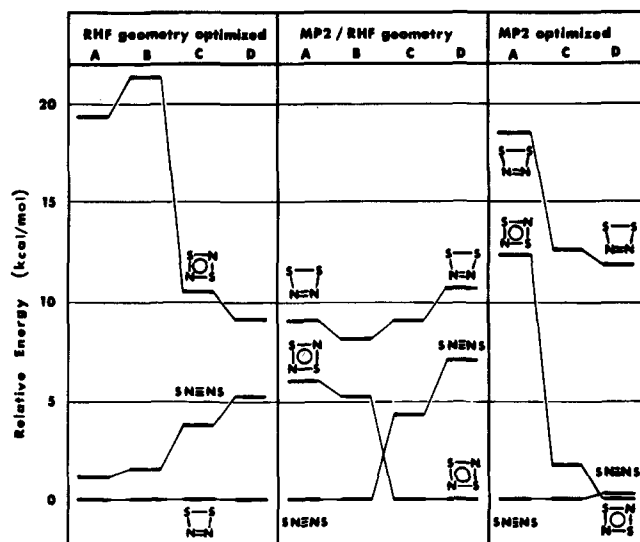


**Figure 6.** Relative energy trends of the three low-energy S<sub>2</sub>N<sub>2</sub> structures as functions of basis set and limited electron correlation. Basis sets: A, 6-31G\*; B, 6-311++G\*; C, 6-311G(2df); D, 6-311++G(3df).

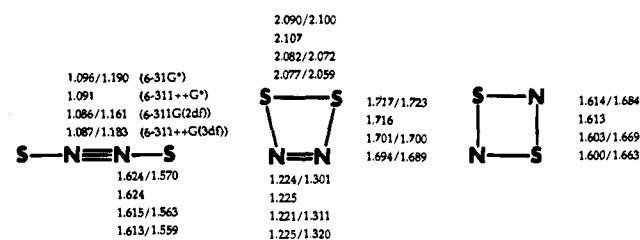


**Figure 7.** Calculated bond distances (in Å) from ab initio calculations for the three low-energy structures. At the top of each stack are the results from basis set A (6-31G\*). In successive lines below are results for B (6-311++G\*), C (6-311G(2df)), and D (6-311++G(3df)). Each line reports the RHF value followed by the MP2 result, RHF/MP2.

provides the only direct comparison of a calculated S<sub>2</sub>N<sub>2</sub> structure with the same structure as determined by experiment. The SN distances (1.651 Å; 1.657 Å) from single-crystal X-ray studies<sup>1,2</sup> fall between the longest calculated value (1.684 Å; MP2/6-31G\*) and the shortest (1.600 Å; RHF/6-311++G(3df)). The calculated value closest to the experimental results comes from the highest level of theory (1.663 Å; MP2/6-311++G(3df)). At the RHF level, calculated bond distances generally contract with increasing quality of the basis set. Differences in individual distances calculated at RHF and MP2 levels with the same basis set are almost independent of basis set. Consider the alternant ring SNSN. If  $\Delta = D(\text{MP2}) - D(\text{RHF})$ ,  $\Delta = +0.070$  Å for 6-31G\*, +0.066 Å for 6-311G(2df), and +0.063

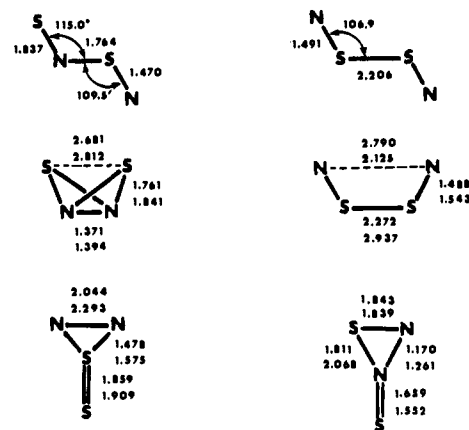


**Figure 8.** Calculated structural parameters (bond distances in Å; bond angles in deg) from 6-31G\* ab initio geometry optimizations for the higher energy structures. In each pair the upper value is the RHF result and the lower member is the corresponding MP2 result. Single values indicate structures that are minima on the RHF surface only.

**Table 2.** Typical Bond Distances (in Å) from a Variety of Experimental Sources

N-N	N=N	N≡N
1.416–1.474 (N <sub>2</sub> H <sub>4</sub> , N <sub>2</sub> H <sub>4</sub> <sup>2+</sup> )	1.167 (H <sub>2</sub> N <sub>2</sub> )	1.098 (N <sub>2</sub> )
S-N	S=N	S≡N
1.705–1.719 (HS-NH <sub>2</sub> )	1.470	1.440 (SN <sup>+</sup> )
1.674 (S <sub>4</sub> N <sub>4</sub> H <sub>4</sub> )	1.54–1.65 (cycles)	
S-S	S=S	
2.02–2.179 (S <sub>6</sub> –S <sub>8</sub> )	1.889 (S <sub>2</sub> )	

Å for 6-311++G(3df). Generally, the MP2 bond distances in Figure 7 are longer than the corresponding RHF values. The difference between RHF and MP2 SN distances in SNSN is more or less typical of bond distance differences at the two levels throughout Figures 7 and 8. But in several instances, differences are 0.25 Å or more. The most dramatic difference occurs for the planar trans NSSN isomer for which the RHF structure has bond distances that are normal compared to typical experimental values, but at the MP2 level, the structure dissociates into two widely separated NS fragments. MP2 optimized structures for both of the Y-shaped isomers as well as for the planar trans NS-SN and planar cis NS-SN chains contain individual bonds that are unrealistically long. However, no anomalous bonds

occur among the three lowest energy structures and we confine our detailed structural descriptions to these three isomers.

At the RHF level the calculated central NN bond distance in the S–N≡N–S linear chain is very much like the N≡N triple bond in N<sub>2</sub>. But at the MP2 level, this bond expands to something closer to an N=N double bond distance. At the RHF and MP2 levels, the flanking NS bonds are too short to be called single bonds; they fall into the range of bond distances found in "aromatic" SN rings. At the MP2 level, the SNNS linear chain could be described by a pair of equivalent resonance structures:

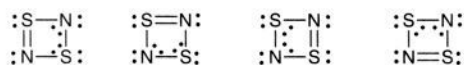


The lone pair on one nitrogen in each structure might also rationalize the minute deviation from strict linearity that we found in this isomer at the MP2 level.

The alternant ring is often pictured as the resonance hybrid of a pair of equivalent valence bond (VB) structures:<sup>34,35</sup>



These structures explain experimental and calculated SN bond distances that are intermediate between standard single and double SN bond distances. Another representation is the set of four equivalent structures:<sup>37,38</sup>



where dots inside the rings indicate electrons in p AOs perpendicular to the plane of the ring and therefore available for  $\pi$  bonding. Using these and several other structures as components of a VB wave function for S<sub>2</sub>N<sub>2</sub>, Harcourt and Skrezenek found the VB component with the greatest weight to be the spin-paired diradical structure with a long N·····N bond:<sup>37,38</sup>



The pairwise ring SNNS is the only one of the three low-energy isomers that can be adequately described by a single canonical Lewis diagram,

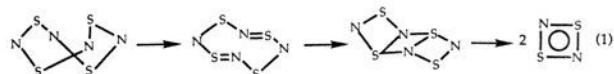


with an N=N double bond, an S–S single bond, and a pair of N–S single bonds. Although we can count six electrons in p AOs perpendicular to the plane of the ring (two from each sulfur and one on each nitrogen) and therefore available as an aromatic sextet, the calculated bond distances show no evidence of delocalized bonding in the pairwise ring.

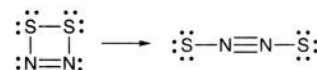
## Discussion

At the most dependable level of theory that we have attempted here, we find the linear SNNS chain and the alternant ring to have the lowest, essentially indistinguishable energies with the

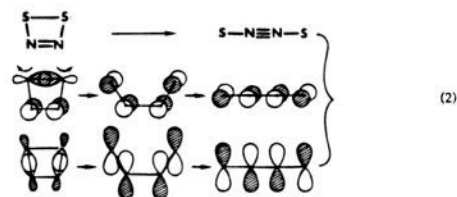
nonalternant ring less than 12 kcal/mol above. The fact that the alternant ring is the only structure that has been firmly established experimentally is probably a result of its synthetic history. S<sub>2</sub>N<sub>2</sub> is commonly prepared through decomposition of the S<sub>4</sub>N<sub>4</sub> cage in which sulfur and nitrogen atoms are already linked together alternately rather than pairwise. Thewalt and Muller speculate that S<sub>4</sub>N<sub>4</sub> decomposes according to eq 1.<sup>39</sup>



If alternant and pairwise 4-membered rings and the SNNS linear chain are the three lowest minima on the S<sub>2</sub>N<sub>2</sub> energy surface, it would be interesting to know what mechanisms might allow them to isomerize to each other. The pairwise ring and the linear SNNS chain have the most obvious connection since both contain NN bonds. Equation 2 shows the breaking of the S–S bond of the ring to give the linear chain with the N≡N triple bond. For the MO pictures the process assumes a disrotating disengagement of AOs in breaking the S–S bond.

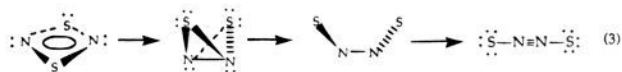


We present a more detailed qualitative MO model of ring-to-



chain changes in a later section.

Conversion of the alternant ring to the SNNS linear chain must be more complicated because a bond must be established between the two nitrogens. One could imagine the formation of an N–N single bond to give a butterfly structure which might then collapse by breaking two S–N bonds, passing through a gauche SNNS chain of C<sub>2</sub> symmetry, to yield the linear chain as shown in eq 3.



Our calculations show that the butterfly structure has an energy that is 35 to 45 kcal/mol higher than that of the planar alternant ring, an energy barrier in itself sufficient to protect the ring from rearranging to the chain through this mechanism. But eq 3 is also unfavorable because it requires a HOMO-LUMO crossing. To form one of the  $\pi$  components of the N≡N triple bond requires utilization of the transannular N–N in-phase combination of p- $\pi$  AOs from the vacant antibonding ring 2a MO. Furthermore, the N–N out-of-phase AO combination in the filled 1b MO must be eliminated. (Here a and b denote MOs as symmetric and antisymmetric, respectively, on rotation about the C<sub>2</sub> axis perpendicular to the plane of the ring.) Figure 9 shows the details. This crossing of filled and empty MOs is a violation of the principle of conservation of orbital symmetry and it must occur somewhere between planar ring and linear chain. An orbital correlation diagram presented by Janssen

(37) Harcourt, R. D.; Skrezenek, F. L. *THEOCHEM* **1987**, 36, 203.

(38) Skrezenek, F. L.; Harcourt, R. D. *J. Am. Chem. Soc.* **1984**, 106, 3934.

(39) Thewalt, J.; Muller, B. Z. *Anorg. Allg. Chem.* **1980**, 462, 214.

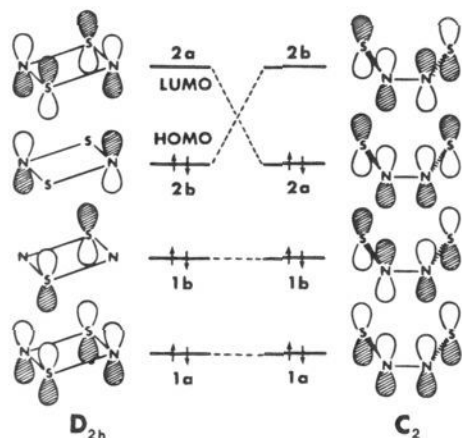
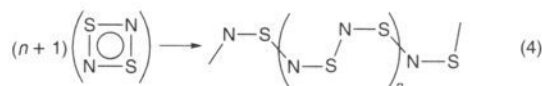


**Figure 9.** Schematic orbital correlations showing the HOMO-LUMO crossing between planar ring and gauche chain. The crossing should stabilize the alternant ring with respect to rearrangement to the SNNS linear chain.

indicates that it occurs between the planar ring and the butterfly.<sup>10</sup> The alternant ring is known to polymerize, eq 4.<sup>1,2,40</sup>



### Vibrational Frequency Results

Hassanzadeh and Andrews observed an infrared absorption peak at 1167.5  $\text{cm}^{-1}$  which they attributed to a new  $\text{S}_2\text{N}_2$  isomer.<sup>25</sup> They note that the SN radical has a peak at 1209  $\text{cm}^{-1}$  in the solid argon matrix and 1204  $\text{cm}^{-1}$  in the gas phase. Table 3 displays the calculated vibrational frequencies and intensities for the three  $\text{S}_2\text{N}_2$  isomeric structures of lowest energy. Among the calculated frequencies of the various  $\text{S}_2\text{N}_2$  isomers, we are looking for something close to 1167.5  $\text{cm}^{-1}$ . Among the calculated frequencies of the three structures of lowest energy, Table 3, there is only one candidate, the  $a_1$  vibration of the pairwise ring  $\overline{\text{SNNS}}$ . The MP2/6-311++G-(3df) value of 1116  $\text{cm}^{-1}$  is slightly smaller than the observed frequency but close enough. Corresponding calculated intensities are substantial.

### Qualitative MO Model

During experiments in which SN radicals were produced, Hassanzadeh and Andrews observed an absorption peak which they attributed to a new isomer of  $\text{S}_2\text{N}_2$ . Using ab initio calculations, we have identified three low-energy isomers of  $\text{S}_2\text{N}_2$ . In this section, we apply qualitative MO arguments to evaluate processes by which SN radicals might combine to yield low-energy  $\text{S}_2\text{N}_2$  isomers and to rationalize the stabilities of linear SNNS and the two  $\text{S}_2\text{N}_2$  rings.

Consider the colinear approach of two diatomic monomer fragments to form a linear symmetric tetraatomic dimer: 2AB  $\rightarrow$  BAAB. Figure 10 is a qualitative MO correlation diagram of valence orbitals for this process. The AO composition diagrams of the diatomic MOs are well-known; those of the linear dimer are easily rationalized as in-phase and out-of-phase combinations of the diatomic fragment MOs with some mixing to be expected among the MOs of  $\sigma$  symmetry. For the separated fragments, the MOs are either doubly degenerate ( $\sigma$  orbitals) or quadruply degenerate (pairs of  $\pi$  orbitals). The order of BAAB energy levels assumed in Figure 10 is very similar to

that obtained by extended Hückel calculations for the 22-valence-electron ion  $\text{O}-\text{C}\equiv\text{C}-\text{O}^{2-}$ .<sup>41</sup> The three A-A bonding orbitals  $2\pi_u$  and  $3\sigma_g$  are easily recognized as those responsible for the  $\text{C}\equiv\text{C}$  triple bond in  $\text{C}_2\text{O}_2^{2-}$ . One can quibble about the details of the order of energy levels of BAAB and surely it will depend on what atomic species are actually involved, but an inspection of MO nodal properties suggests that the 22-electron HOMO ( $2\pi_u$ ) and all MOs below it should be lower in energy than the LUMO ( $2\pi_g$ ), an arrangement crucial to the following arguments. Imagine two 11-electron SN fragments coming together to form the  $\text{S}-\text{N}\equiv\text{N}-\text{S}$  dimer. On the fragment side of Figure 10, the levels are completely filled through  $1\pi_g$ ,  $1\pi_u$  and the  $2\pi_u$ ,  $2\pi_g$  orbitals hold two unpaired electrons. On dimerization electrons from the fragments do not flow smoothly into the lowest available levels of the dimer. Orbital symmetry requirements direct a pair of electrons from the  $3\sigma_u$  level of the monomers to the dimer antibonding  $3\sigma_u$  level high above the 22-electron HOMO  $2\pi_u$ , which in this case ends up only half filled. The direct colinear dimerization of two SN to form linear symmetric SNNS is not allowed by the principle of conservation of orbital symmetry.

Next, imagine the coplanar, side-by-side approach of two 11-electron SN fragments to form the nonalternant or pairwise ring  $\overline{\text{SNNS}}$ . In constructing Figure 11, the qualitative MO correlation diagram for this process, we assumed the approach follows  $C_{2v}$  symmetry with MOs classified as  $a_1$ ,  $a_2$ ,  $b_1$ , and  $b_2$ . Each SN fragment would have a single electron in one of the antibonding p MOs,  $5a_1$ ,  $5b_2$ ,  $2a_2$ , or  $2b_1$ . AO composition diagrams of ring MOs are highly stylized to suggest fragment MO parentage. Actual MOs involve considerable mixing. In the 22-electron ring the HOMO should be  $5a_1$ . Under  $C_{2v}$  symmetry, MOs of the diatomic fragment and the ring dimer are connected by lines in Figure 11. These connections show that the coplanar  $C_{2v}$  dimerization process is symmetry forbidden, electrons in the  $4b_2$  MO of the fragments going into the high-energy  $4b_2$  orbital of the ring, far above the HOMO  $5a_1$ .

Simple modification of Figure 11 reveals that the noncoplanar  $C_2$  approach of two SN units is allowed. Under  $C_2$  symmetry MOs are classified either as a or b, symmetric or antisymmetric with respect to the same  $C_2$  axis as in  $C_{2v}$ . Under the less stringent requirements of  $C_2$  symmetry, 22 electrons from the fragment pair flow directly into the lowest energy MOs of the nonplanar ring which could then collapse to the lower energy planar structure.

The coplanar, parallel approach of two SN fragments to form the alternant ring  $\overline{\text{SNSN}}$  would be  $C_{2h}$  symmetry. With a little imagination, the MOs of Figure 11 can be reclassified as  $a_g$ ,  $a_u$ ,  $b_g$ , and  $b_u$ . The pattern of connections among levels shows that 22 valence electrons from two SN fragments flow smoothly into the lowest available MOs of the alternant ring for a symmetry-allowed dimerization.

From qualitative MO arguments, we conclude that the formation of the linear SNNS dimer from colinear approach of SN radicals is symmetry forbidden. Plausible approaches of SN fragments to form rings are symmetry allowed, although the noncoplanar  $C_2$  process that leads to the nonalternant  $\overline{\text{SNNS}}$  ring is not as straightforward as the coplanar parallel  $C_{2h}$  process that gives the alternant  $\overline{\text{SNSN}}$  ring. Therefore, we still cannot unambiguously explain the experimental results of Hassanzadeh and Andrews, who do not observe the alternant ring; the absorption which they observe matches what we would expect for the nonalternant ring.

(40) Boudeulle, M. *Cryst. Struct. Commun.* **1975**, *4*, 9.

(41) Gimarc, B. M. *J. Am. Chem. Soc.* **1970**, *92*, 266.



**Table 3.** Calculated Vibrational Frequencies (cm<sup>-1</sup>) for the Three Low-Energy Isomers of S<sub>2</sub>N<sub>2</sub><sup>a</sup>

method/basis set	S—N=N—S						S—N≡N—S								S—N   O—N   S			
	a <sub>2</sub>	a <sub>1</sub>	b <sub>2</sub>	a <sub>1</sub>	b <sub>2</sub>	a <sub>1</sub>	π <sub>u</sub>	σ <sub>g</sub>	π <sub>g</sub>	σ <sub>u</sub>	σ <sub>g</sub>	b <sub>3u</sub>	b <sub>1u</sub>	a <sub>g</sub>	b <sub>2u</sub>	b <sub>3g</sub>	a <sub>g</sub>	
MP2/6-311G(2df)	494 (0)	516 (9.7)	481 (1.5)	744 (26.4)	851 (6.1)	1143 (44.7)	159 (0)	546 (0)	225 (0)	1032 (43.3)	1942 (31.4)	472 (20.5)	770 (14.4)	626 (0)	793 (2.3)	880 (0)	839 (0)	
MP2/6-311++G(3df)	499 (0)	516 (9.9)	500 (0.4)	771 (18.7)	859 (34.8)	1116 (39.6)	152 (0)	551 (0)	116 (0)	1037 (39.7)	1910 (0)	475 (17.1)	783 (17.6)	620 (0)	791 (7.1)	886 (0)	851 (0)	

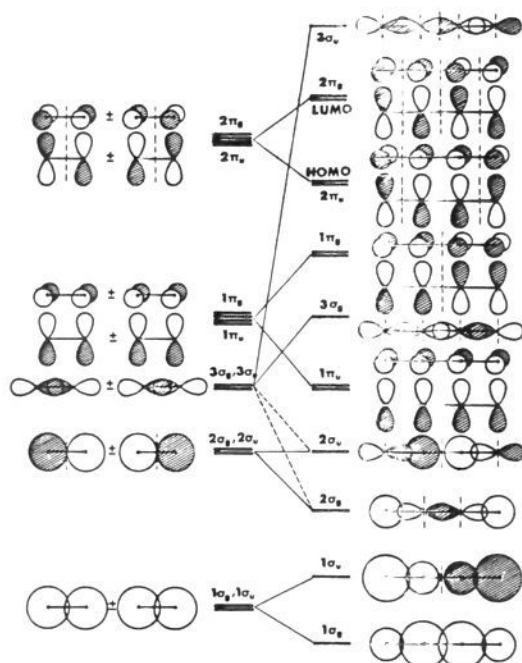
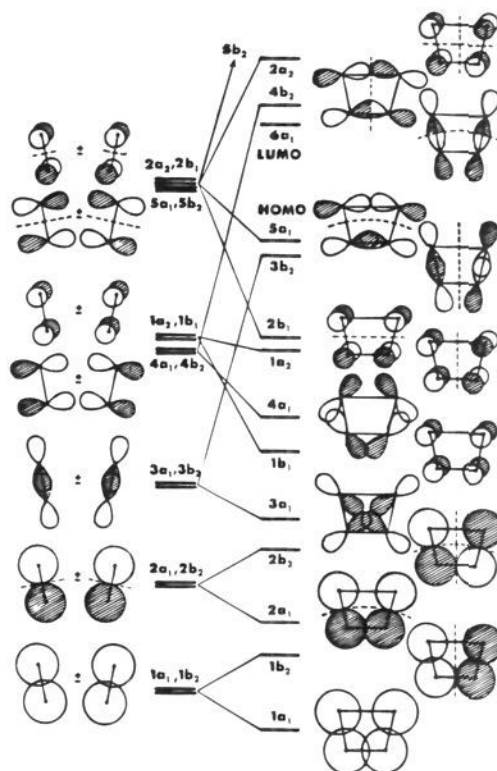
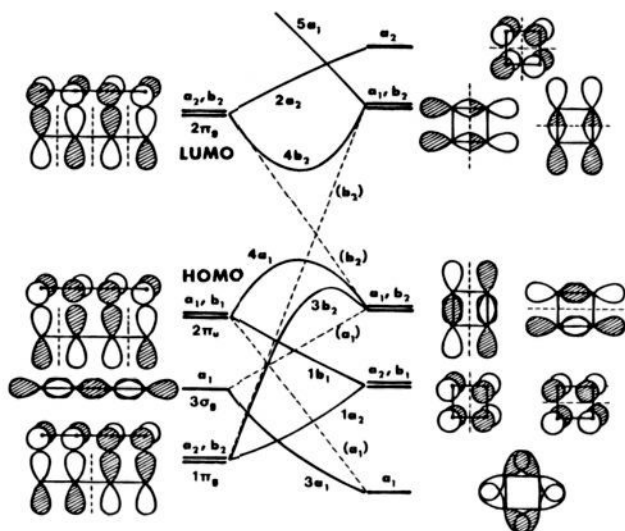
<sup>a</sup> Calculated intensity appears in parentheses below each frequency.**Figure 10.** Schematic valence MO correlation diagram for the colinear dimerization of AB fragments to form the linear symmetric dimer BAAB. At the 22-electron level (S<sub>2</sub>N<sub>2</sub>) the dimer HOMO is 2π<sub>u</sub>. Dashed lines indicate mixing of orbitals of similar symmetry (σ<sub>g</sub> or σ<sub>u</sub>).

Figure 12 is a highly schematic correlation diagram showing AO compositions and nodal properties of several MOs on either side of the HOMO-LUMO gap for linear and square shapes of the typical 22-valence-electron tetraatomic molecule BAAB. This diagram was developed from an earlier qualitative MO model which in turn was based on AO compositions and relative MO energies from extended Hückel calculations for C<sub>2</sub>O<sub>2</sub><sup>2-</sup>.<sup>41</sup> The six valence MOs at lower energy do not appear in Figure 12. Except for familiar σ and π designations for MOs of linear geometry, the symmetry classifications (a and b) are those of the intervening planar cis structure of C<sub>2v</sub> symmetry. The acetylenic triple bond between the central pair of atoms of the linear structure can be recognized through the bonding or in-phase overlaps of adjacent AOs in the 3σ<sub>g</sub> and 2π<sub>u</sub> MOs. Dashed lines indicate MO correlations that are "intended" in the sense that comparable AO compositions and overlap phase relations lead one to expect one MO to convert into the other as shape changes. These intended correlations are not realized, however, because MOs of the same symmetry must connect as dictated by energy order and without crossing each other. For example, AO composition of the b<sub>2</sub> component of the 2π<sub>g</sub> LUMO would logically produce the b<sub>2</sub> HOMO of the square, but the energy order of b<sub>2</sub> orbitals requires that it connect with the b<sub>2</sub> LUMO of the square. Similarly, the b<sub>2</sub> component of 1π<sub>g</sub> intends to become the b<sub>2</sub> LUMO of the square or an even

**Figure 11.** Schematic valence MO correlation diagram for the dimerization of AB fragment to form the BAAB ring. The coplanar C<sub>2v</sub> approach is symmetry forbidden for 22 electrons.

higher energy orbital but instead it must connect with the square b<sub>2</sub> HOMO. On bending from linear to square, these two b<sub>2</sub> MOs, initially rather far apart in energy, may start toward each other but then mix and diverge as shown for 3b<sub>2</sub> and 4b<sub>2</sub> in Figure 12. The behavior of the MOs 3a<sub>1</sub> and 4a<sub>1</sub> is related but slightly different. Lying close together in linear geometry, as 3σ<sub>g</sub> and a component of 2π<sub>u</sub>, on bonding, these two a<sub>1</sub> MOs must actually mix to give the lowest 3a<sub>1</sub> MO of the ring. As a result, these two MOs may spread apart, as shown at intermediate geometry, before changing course to correlate with ring orbitals of appropriate energy order.

Since the HOMO 4a<sub>1</sub> rises in energy on cis bending from linear 2π<sub>u</sub>, one would expect 22-electron BAAB molecules to be linear rather than planar cis. As shown in Figure 12, the 4a<sub>1</sub> hump serves as an energy barrier separating linear from planar ring forms. Indeed, we find both linear SNNS and SNNS ring shapes are real minima at RHF and MP2 levels for all basis sets considered here. If 2π<sub>u</sub> and 2π<sub>g</sub> levels are close in energy, 4b<sub>2</sub> might actually cross and dip below 4a<sub>1</sub>, making 4b<sub>2</sub> the HOMO and stabilizing planar cis geometry. Notice that 2π<sub>u</sub> is AA bonding and 2π<sub>g</sub> is AA antibonding. A short, strong AA bond will therefore have a large HOMO-LUMO gap by



**Figure 12.** Schematic correlations of MOs near the HOMO-LUMO gap connecting the linear chain and the square ring. Labels  $a_1$ ,  $a_2$ ,  $b_1$ , and  $b_2$  reflect symmetry classifications assuming  $C_{2v}$  symmetry for the connecting cis-bent structure. Dashed lines indicate unrealized intended correlations based on related AO compositions of MOs.

increasing the in-phase interactions between adjacent  $p-\pi$  AOs in  $2\pi_u$  and out-of-phase overlaps in  $2\pi_g$ . Such a situation might be expected in SNNS with a particularly strong  $N\equiv N$  triple bond. The result would be stable linear SNNS separated from

the SNNS ring by the  $4a_1$  energy barrier. But if the central AA bond is weak, then the HOMO-LUMO gap is small and  $4b_2$  might dip below  $4a_2$  (as it does in Figure 15 of ref 41). The electron pair, formerly occupying the AA-bonding  $4a_1$  MO, now resides in the AA-antibonding  $4b_2$  orbital, reducing the qualitative AA bond order from 3 to 1 and stabilizing the planar cis conformation as is the case for the experimental structure of ONNO and our calculated structure of NSSN. In these situations, the HOMO-LUMO crossings of  $4a_1$  and  $4b_2$  would separate planar cis NSSN from the ring NSSN.

## Conclusions

The planar alternant ring SNSN has long been known but a recent matrix isolation infrared spectroscopic study suggests that another  $S_2N_2$  isomer may be stable. From geometry optimized ab initio calculations we have found nine structural isomeric forms that are relative minima on the  $S_2N_2$  energy surface at the RHF/6-31G\* level. Further calculations for these structures establish that at least seven of these forms are minima on the MP2/6-31G\* surface as well. Within both RHF and MP2 approximations three structures have the lowest energies: the SNNS linear chain and the 4-membered rings SNSN and SNNS. Geometry optimized calculations at the MP2/6-311++G(3df) level give almost identical energies for the linear chain SNNS and the alternant ring SNSN with the nonalternant or pairwise ring SNNS less than 12 kcal/mol above. Single-point MP4 calculations reduce energy differences among these isomers to 2.5 kcal/mol. Calculated bond distances in the three structures of lowest energy can be rationalized by traditional VB and MO models. Calculated vibrational spectra give one frequency from the pairwise SNNS ring that matches perfectly with the matrix isolation frequency that has been reported and attributed to a new isomer of  $S_2N_2$ . A qualitative MO model suggests that colinear dimerization of SN radicals to form linear symmetric SNNS is symmetry forbidden but dimerization processes leading to both rings are allowed. The qualitative MO model can also rationalize relative minima found for linear SNNS, cis NSSN, and the pairwise ring SNNS.

**Acknowledgment.** We are grateful to the National Science Foundation for partial support of this research through Grant No. CHE-9012216 to the University of South Carolina. D. S. Warren is pleased to acknowledge a U.S. Department of Education graduate fellowship awarded to him through the Department of Chemistry and Biochemistry at the University of South Carolina.

JA9425804